Virus Research 340 (2024) 199296

Contents lists available at ScienceDirect

Virus Research

journal homepage: www.elsevier.com/locate/virusres

LysZX4-NCA, a new endolysin with broad-spectrum antibacterial activity for topical treatment

Ping Li [a], Mangmang Shen [a], Wenjie Ma [a], Xin Zhou [a,b,c,*], Jiayin Shen [d,*]

[a] College of Veterinary Medicine, Institute of Comparative Medicine, Yangzhou University, Yangzhou 225009, PR China
[b] Jiangsu Co-innovation Center for Prevention and Control of Important Animal Infectious Diseases and Zoonoses, Yangzhou University, Yangzhou 225009, PR China
[c] Joint International Research Laboratory of Agriculture and Agri-Product Safety, the Ministry of Education of China, Yangzhou University, Yangzhou 225009, PR China
[d] The Third People's Hospital of Shenzhen, Shenzhen 518112, PR China

ARTICLE INFO

Keywords:
Klebsiella pneumoniae
Phage
Endolysin
Outer membrane
Broad spectrum

ABSTRACT

The prevalence of multidrug-resistant highly virulent *Klebsiella pneumoniae* (MDR-hvKP) requires the development of new therapeutic agents. Herein, a novel lytic phage vB_KpnS_ZX4 against MDR-hvKP was discovered in hospital sewage. Phage vB_KpnS_ZX4 had a short latent period (5 min) and a large burst size (230 PFU/cell). It can rapidly reduce the number of bacteria *in vitro* and improve survival rates of bacteremic mice *in vivo* from 0 to 80 % with a single injection of 10^8 PFU. LysZX4, an endolysin derived from vB_KpnS_ZX4, exhibits potent antimicrobial activity *in vitro* in combination with ethylenediaminetetraacetic acid (EDTA). The antimicrobial activity of LysZX4 was further enhanced by the fusion of KWKLFKI residues from cecropin A (LysZX4-NCA). *In vitro* antibacterial experiments showed that LysZX4-NCA exerts broad-spectrum antibacterial activity against clinical Gram-negative bacteria, including MDR-hvKP. Moreover, in the mouse model of MDR-hvKP skin infection, treatment with LysZX4-NCA resulted in a three-log reduction in bacterial burden on the skin compared to the control group. Therefore, the novel phages vB_KpnS_ZX4 and LysZX4-NCA are effective reagents for the treatment of systemic and local MDR-hvKP infections.

1. Introduction

The species *Klebsiella pneumoniae*, a Gram-negative pathogen, is generally divided into opportunistic, hypervirulent, and multidrug-resistant groups according to its large number of accessory genes of plasmids and chromosomal gene loci (Martin and Bachman, 2018). As the second most opportunistic pathogen in nosocomial infections, *K. pneumoniae*, especially highly virulent *K. pneumoniae* (hvKP) (Tutelyan et al., 2022) and multidrug resistant *K. pneumoniae* (MDR-KP) (Calfee, 2010), tends to infect critically ill people with defective immune functions, causing pneumonia, urinary tract infections, burn infections, bacteremia, and other complications (Podschun and Ullmann, 1998). Through horizontal gene transfer, the recombination and selection processes can lead to the emergence of multidrug-resistant highly virulent *K. pneumoniae* (MDR-hvKP), wherein virulence and resistance genes coexist within the same bacteria (Tang et al., 2020). The diminishing efficacy of antibiotics against MDR-hvKP has consequently amplified the demand for non-antibiotic alternatives (Pusparajah et al., 2022).

Bacteriophages, also known as phages, are viral entities that specifically infect bacteria and represent a highly abundant group of organisms on Earth (Keen, 2015). Due to their remarkable host specificity, rapid bactericidal activity, and minimal impact on the human body, phages have emerged as a promising alternative to conventional antibiotics. Mounting evidence suggests that phage therapy exhibits exceptional efficacy in treating various infections caused by *K. pneumoniae* in animal models and clinical cases including pneumonia (Anand et al., 2020), liver abscesses (Hung et al., 2011), burn infections (Kumari et al., 2009), urinary tract infections (Qin et al., 2020), bacteremia (Hesse et al., 2021), and medical equipment-associated infections. However, limited attention has been given to the exploration of phages against hvKP, particularly MDR-hvKP (Anand et al., 2020; Gorodnichev et al., 2021; Wang et al., 2021). Therefore, there is an urgent need for isolation of additional phages targeting MDR-hvKP.

Compared to the phage itself, the phage derivative endolysin can be more easily standardized for production and application as an alternative antibacterial agent. Endolysin functions by degrading the peptidoglycans of cell walls during the late stage of phage proliferation,

* Corresponding author.
E-mail addresses: zhou_xin@126.com (X. Zhou), shenjiayin@shphc.org.cn (J. Shen).

https://doi.org/10.1016/j.virusres.2023.199296
Received 13 February 2023; Received in revised form 2 December 2023; Accepted 5 December 2023
Available online 8 December 2023

resulting in progeny release (Chamblee et al., 2022; Wang et al., 2021). Previous studies have demonstrated that endolysin exhibits potent antibacterial activity against multidrug resistant pathogens, especially against Gram-positive bacteria (Fischetti, 2018; Ghose and Euler, 2020; Ho et al., 2022). Endolysin generally displays higher sensitivity towards Gram-positive bacteria, where the peptidoglycan layer is exposed, as the peptidoglycan layer of Gram-negative bacteria is covered by the outer membrane (OM). To overcome the OM barrier and effectively target with endolysins, various strategies have been employed such as identifying endolysins capable of penetrating through the OM or modifying them with high charge/hydrophobic amino acid residues. Additionally, formulating endolysins with nanocarriers or utilizing them together with an OM permeating agent has also been explored (Lai et al., 2020). Endolysins derived from *K. pneumoniae* phages have received little attention thus far, with only three reported examples demonstrating antibacterial activity: LysG24 (Lu et al., 2022), KP27 endopeptidase (Maciejewska et al., 2017) and KP32gp15 (Walmagh et al., 2013). In this study, we reported B_KpnS_ZX4 targeting MDR-hvKP along with a comprehensive analysis of its biological properties. Furthermore, we expressed and tested the antibacterial activity of LysZX - an endolysin derived from vB_KpnS_ZX4 - using prokaryotic cells. Finally, we evaluated the antibacterial activity of vB_KpnS_ZX4 and its corresponding endolysin against multidrug resistant MDR-hvKP infected mice.

2. Materials and methods

2.1. Bacterial strains

K. pneumoniae used in this study was isolated from a clinical sample (Yangzhou, China) and grown in Luria-Bertani (LB) at 37 °C. Primers K1-F/R to K57-F/R, rmpA-F/R to wabG-F/R, and CTX-M1-F/R to SHV-F/R were used to identify capsular serotypes, virulence genes, and drug-resistance genes, respectively. Multi-locus sequence typing (MLST) was performed using the primers provided by the Institut Pasteur MLST (https://bigsdb.pasteur.fr/klebsiella/). Primers used in this study are listed in Table S1.

2.2. Phage isolation and host range

Sewage samples were collected from hospitals (Yangzhou, China), and phage vB_KpnS_ZX4 was isolated with *K. pneumoniae* O4 as the host. After 3 single-plaque passages the phages were enriched by PEG/NaCl, as previously described (Li et al., 2021). The phage morphology was observed using a transmission electron microscope (TEM) JEM-1200EX (Jeol Ltd., Tokyo, Japan) by staining with 2 % phosphotungstic acid. Seven clinical isolates of *K. pneumoniae* stored in our laboratory were used to determine the host range of the phage vB_KpnS_ZX4.

2.3. Phage biological properties

The one-step growth curve of the phage was determined at a multiplicity of infection (MOI) of 0.1 (Li et al., 2022). Logarithmic-phase cells of *K. pneumoniae* O4 and vB_KpnS_ZX4 were incubated at 37 °C for 10 min, followed by removal of unbound phages from the supernatant. The bacterial precipitate was resuspended in LB medium and incubated at 37 °C with agitation at 220 rpm. The phage titer in the culture was assessed every 5 min. The thermal tolerance and pH sensitivity assays were conducted by subjecting vB_KpnS_ZX4 (10^8 PFU/mL) to temperatures ranging from 4 to 80 °C and pH values spanning from 2.0 to 14.0 using buffer solutions for a duration of 1 h, respectively (Li et al., 2022). The killing kinetics of the phage were determined by monitoring changes in bacterial numbers upon addition of vB_KpnS_ZX4 with different MOIs (10, 1, and 0.1) to logarithmic-phase *K. pneumoniae* O4 cultures maintained at a temperature of 37 °C with agitation at a speed of 220 rpm (Li et al., 2022).

2.4. Phage genome characteristics

The genome of phage vB_KpnS_ZX4 was extracted, sequenced, assembled, and analyzed following previously described methods (Li et al., 2021). Genome analysis encompassed tRNA prediction (Chan et al., 2021), virulence gene prediction (Liu et al., 2019), drug resistance gene prediction (Alcock et al., 2020), open reading frame (ORF) annotation (Overbeek et al., 2014), and genome sequence similarity analysis using the reported methodologies (Sullivan et al., 2011). Protein analyses included sequence similarity analysis using MEGA 5.0, conservative domain analysis as described by Lu et al. (Lu et al., 2020), transmembrane structure prediction with TMHMM-2.0, signal peptide prediction employing SignalP-5.0, as well as secondary and three-dimensional structure prediction based on Kelley et al.'s approach (Kelley et al., 2015).

2.5. Endolysin expression and purification

The PCR products of LysZX4 and pET28a were amplified using Champagne Taq DNA Polymerase (Vazyme, Nanjing, China) with the primers LysF/R and 28a-F/R. The purified DNA products were connected using the ClonExpress II One Step Cloning Kit (Vazyme). Competent *E. coli* BL21 (DE3) cells were transformed with the attached plasmid. The positive plasmid pET28a-LysZX4 was amplified using T7-F/R primers and confirmed by Sanger sequencing. Similarly, mutant plasmids of LysZX4, namely pET28a-LysZX4-39/41 (A39T, S41I), pET28a-LysZX4-52 (A52V), pET28a-LysZX4-74 (S74A), PET28a-LysZX4-108/109 (S108A, C109R), and pET28a-LysZX4-141 (Q141E), were constructed using the primers LysF/R-39/41, LysF/R-52, LysF/R-74, LysF/R-108/109, and LysF/R-141, respectively.

Cecropin is an amphiphilic peptide secreted by insects that is rich in hydrophobic and cationic amino acids (Hancock and Chapple, 1999). Residues 1–8 (KWKLFKI) of cecropin A antibacterial peptide have been reported to enhance of endolysin penetration through the OM (Lu et al., 2022). The plasmids pET28a-LysZX4-NCA displaying residues KWKLFKI at the N-terminus and pET28a-LysZX4-CCA displaying residues KWKLFKI at the C-terminus were constructed using primers LysF/R-NCA and LysF/R-CCA with the pET28a-LysZX4 vector as a template. Plasmid pET32a-LysZX4 was also constructed using primers LysF2/R2 and 32a-F/R and the pET32a vector used as a template. Additionally, plasmid pET32a-LysZX4-NCA was generated by employing primers LysF3/R3 using the pET32a-LysZX4 plasmid as a PCR template.

Isopropyl-β-d-thiogalactopyranoside (IPTG) (0.5 mM) was added to log-phase *E. coli* BL21 (DE3) cells containing a positive plasmid, and then the cells were cultured for 24 h at 16 °C to induce expression of the recombinant protein. The separation, purification, and quantification of recombinant proteins were performed as previously described (Li et al., 2021). Briefly, overnight cultured bacteria were centrifuged and resuspended in PBS. The suspensions were sonicated and centrifuged. The lysates were then passed through a gravity column, and the recombinant proteins were eluted with 150 mM imidazole buffer. The collected recombinant proteins were purified and concentrated using 10 KDa ultrafiltration tubes, and the concentration was determined using a BCA protein quantification kit (Vazyme).

Finally, we obtained the following highly pure recombinant endolysins: endolysin LysZX4; endolysin mutants LysZX4-39/41, LysZX4-52, LysZX4-74, LysZX4-108/109, and LysZX4-141; engineered endolysin LysZX4-NCA expressed by the pET28a plasmid, and LysZX4-NCA (pET32a) expressed by the pET32a plasmid. The purified endolysin was subjected to sodium dodecyl sulfate-polyacrylamide gel electrophoresis (SDS-PAGE) and stained with Coomassie Brilliant Blue for visualization. For Western blotting analysis, the purified endolysin was transferred onto a PVDF transfer membrane (Merck KGaA, Darmstadt, Germany), incubated with 5 % PBSA for 2 h followed by anti-His-Tag mouse monoclonal antibody (Cwbio, Taizhou, China) for another 2 h. Subsequently, it was incubated with goat anti-mouse IgG conjugated to

horseradish peroxidase (Cwbio) for 1 h. Immunoreactive protein bands were detected using an electrochemiluminescence detection system (Tanon, Shanghai, China).

2.6. In vitro antibacterial activity of endolysin

The effect of EDTA on the antibacterial activity of LysZX4 was assessed. To evaluate the antibacterial activity of endolysin, the *K. pneumoniae* O4 were resuspended in PBS buffer followed by centrifugation. Log-phase (OD_{600}=0.6) or stationary-phase (OD_{600}=1.2) cells at a final concentration of 5×10^8 CFU/mL, LysZX4 at a final concentration of 100 μg/mL, and EDTA at final concentrations ranging from 0 to 10 mM (0, 0.05, 0.1, 0.5, 1, 5, and 10 mM) were added to individual wells in a 96-well plate (200 μL per well). Three parallel wells were included for each condition and incubated at 37 °C for duration between 1 and 6 h. Bacterial counts were determined hourly using plating techniques.

The antibacterial activity of the engineered endolysin in the presence of EDTA was determined. Log-phase cells of *K. pneumoniae* O4 at a final concentration of 5×10^8 CFU/mL, EDTA with a final concentration of 1 mM, and LysZX4, LysZX4–39/41, LysZX4–52, LysZX4–74, LysZX4–108/109, LysZX4–141, LysZX4-NCA, LysZX4-CCA, LysZX4 (pET32a), and LysZX4-NCA (pET32a) at a final concentration of 100 μg/mL were added to 96-well plates (200 μL per well). PBS was used as a blank control instead of endolysin. Following incubation at 37 °C for 1–6 h, bacterial counts were determined every hour.

The optimal antibacterial concentration for LysZX4-NCA was determined using log-phase cells of *K. pneumoniae* O4 at a final concentration of 5×10^8 CFU/mL and EDTA at a final concentration of 1 mM. Different concentrations (0, 5, 10, 50, 100, and 500 μg/mL) of LysZX4 were added to individual wells in a 96-well plate (200 μL per well). After incubation at 37 °C for 1–6 h, bacterial counts were determined every hour.

The antibacterial activity of LysZX4-NCA against bacteria in the logarithmic and stationary phases was determined. Log-phase or stationery-phase cells of *K. pneumoniae* O4 at a final concentration of 5×10^8 CFU/mL, EDTA at a final concentration of 1 mM, and LysZX4-NCA at a final concentration of 100 μg/mL were added into 96-well plates (200 μL per well). After incubation at 37 °C for 1–6 h, the bacterial count was assessed every hour.

The antibacterial activities of LysZX4-NCA against 16 clinical isolates, including *K. pneumoniae, Escherichia coli, Proteus mirabilis*, and *Citrobacter*, were determined. These clinical isolates were obtained from sewage samples collected from the Affiliated Hospital of Yangzhou University (Yangzhou, China). Log-phase cells of bacteria at a final concentration of 10^8 CFU/mL, LysZX4-NCA at a final concentration of 100 μg/mL, and EDTA at a final concentration of 1 mM or PBS, were added to each well in the 96-well plates (200 μL per well). After incubation at 37 °C for 4 h, the bacterial count in each well was determined using plate coating.

2.7. TEM analysis of endolysin-treated K. pneumoniae

Log-phase cells of *K. pneumoniae* O4 were resuspended in PBS, and the treatment group was supplemented with LysZX4 or LysZX4-NCA (100 μg/mL) along with EDTA (1 mM), while the control group received an equal volume of PBS or EDTA (1 mM). All groups were incubated at 37 °C for 2 h. Subsequently, the bacteria were washed three times with PBS. The treated bacteria were fixed with 2.5 % glutaraldehyde for 4 h and negatively stained using 2 % phosphotungstic acid. Finally, the morphology of the bacteria was observed by TEM.

2.8. Stability of endolysin

The LysZX4-NCA (100 μg/mL) was incubated at temperatures of 30, 37, 45, 55, 65, and 75 °C for 1 h. Subsequently, it was added to log-phase cells of *K. pneumoniae* O4 (5×10^8 CFU/mL) for incubation at 37 °C for 4 h. The thermal stability of LysZX4-NCA was determined by calculating the ratio of the bactericidal quantity at different temperatures to the sterilization quantity at 37 °C.

The Log-phase cells of *K. pneumoniae* O4 (5×10^8 CFU/mL) were resuspended in buffers with varying pH values, and then incubated at 37 °C for 4 h after the addition of LysZX4-NCA. The pH stability of LysZX4-NCA was determined by calculating the ratio of the bactericidal quantity at different pH buffers to the sterilization quantity at pH=7.0.

The Log-phase cells of *K. pneumoniae* O4 (5×10^8 CFU/mL) were resuspended in serum at concentrations ranging from 0 to 20 %. Subsequently, LysZX4-NCA was added and the mixture was incubated at 37 °C for 4 h. The effect of serum on LysZX4-NCA was determined by the ratio of the bactericidal quantity at different serum contents to the sterilization quantity in PBS buffer. Mouse serum was obtained by centrifuging specific-pathogen-free (SPF) female BABL/C mice blood for 10 min after precipitation for 2 h at 37 °C.

2.9. In vivo antibacterial activity of vB_KpnS_ZX4 and LysZX4-NCA

Animal experiments were conducted on 6-week-old female SPF BABL/C mice (18–20 g) obtained from the Experimental Animal Center of Yangzhou University. The mice were randomly divided into 13 groups, each group consisting of 5 mice. The *in vivo* antibacterial efficacy of phage vB_KpnS_ZX4 was evaluated using a mouse bacteremia model. Group A: Mice were injected intraperitoneally with PBS in a volume of 100 μL. Group B: Mice were injected intraperitoneally with vB_KpnS_ZX4 of 10^9 PFU in a volume of 100 μL. Group C-G: Mice were first injected intraperitoneally with *K. pneumoniae* O4 at 10^7 CFU in a volume of 100 μL, and then the bacterial titers (bacteria count per gram) in blood and organs of mice were measured at five time points 1 h (Group C), 3 (Group D), 6 (Group E), 12 (Group F), and 24 h (Group G) post-infection. Group H-J: All mice were infected intraperitoneally with *K. pneumoniae* O4 at a concentration of 10^7 CFU in a volume of 100 μL, and then injected with 100 μL of phage vB_KpnS_ZX4 with a concentration of 10^9 PFU at 1 h (Group H), 3 h (Group I), and 6 h (Group J) post-infection, respectively. The survival rates of the mice were recorded for 5 days. Blood samples and major organs of mice infected with bacteria were collected to determine the bacterial load. Blood samples were diluted with PBS gradient immediately after sampling. Organ samples were first homogenized with 1 mL PBS and then diluted with PBS gradient. The bacterial load in blood and organ homogenates was determined by plate counting. The *in vivo* antibacterial activities of LysZX4-NCA were evaluated using a mouse skin infection model (Pastagia et al., 2011). The dorsal skin of the mice was depilated, and the top layers of the epidermis were gently removed by peeling with adhesive tape. Subsequently, the skin was infected with *K. pneumoniae* O4 at a concentration of 10^8 CFU per cubic centimeter. After 20 h of bacterial colonization, 200 μg of LysZX4-NCA or PBS was used as a control. After 4 h of treatment, the infected skins were excised, weighed, and homogenized in 1 mL of PBS to determine the bacterial load.

2.10. Statistical analysis

The phage biological property tests, phage *in vitro* antibacterial tests, and endolysin *in vitro* antibacterial tests were repeated 3 times. All statistical analyses were performed using GraphPad Prism 5 software with unpaired *t*-tests. Significance analyses were performed with $P < 0.05$ (*), $0.01 < P < 0.05$ (**), $0.001 < P < 0.01$ (***), and $P < 0.001$ (****).

3. Results

3.1. Phage vB_KpnS_ZX4

K. pneumoniae O4 with a hypermucoviscous phenotype (Fig. S1) was identified as ST608 and K1 capsular serotypes. *K. pneumoniae* O4 encoded nine virulence genes: *rmpA, allS, ureA, fimH, ybtA, iroNB, kfuBC,*

wabG and *wcaG* (Table 1). *K. pneumoniae* O4 encoded *SHV-1* β-lactamase and was resistant to ampicillin, tobramycin, sulfamethoxazole, erythromycin, and azithromycin (Table S2). The phenotypes of high virulence and multiple drug resistance indicated that *K. pneumoniae* O4 belongs to the MDR-hvKP family.

Phage vB_KpnS_ZX4 had an icosahedral head with a diameter of 55 ±2 nm, a tail with a length of 150±2 nm (Fig. 1a), and could form small and translucent plaques with a diameter of 0.7 ± 2 mm on *K. pneumoniae* O4 (Fig. 1b). Phage vB_KpnS_ZX4 showed lytic activity only against *K. pneumoniae* O4 and could not successfully infect the other seven clinical isolates of *K. pneumoniae* (Table 1).

3.2. Biological properties of vB_KpnS_ZX4

Fig. 2a illustrates that phage vB_KpnS_ZX4 exhibited a latent period (L) of 5 min and a burst size (B) of approximately 230 PFU/cell. Fig. 2b shows a slight decrease between 37 °C and 50 °C. Above 50 °C the activity decreased rapidly and was completely lost at 70 °C. The optimal pH for vB_KpnS_ZX4 was found to be between pH 4.0 and pH 9.0, as shown in Fig. 2c; however, complete inactivation occurred at pH values of either 2.0 or 13.0. Furthermore, as depicted in Fig. 2d, phage vB_KpnS_ZX4 significantly reduced bacterial numbers within the first 2 h post-infection proportional to the number of phages used. The effective time of phage vB_KpnS_ZX4 to control bacteria was 2 h, which was similar to the reported results of phages BUCT541 and BUCT610 with high homologous genomes to vB_KpnS_ZX4 (Pu et al., 2022a, 2022b).

3.3. Genomic analysis of vB_KpnS_ZX4

The phage vB_KpnS_ZX4 (accession number MW722082) possessed a double-stranded DNA consisting of 45,424 bp, exhibiting a GC content of 48.37 %. A total of 72 open reading frames (ORFs) and three tRNAs were annotated, among which 17 ORFs (24 %) exhibited speculative functions (Table S3). The primary ORFs associated with nucleic acid metabolism (ORF27, ORF29, ORF30, ORF54, ORF55, ORF57, ORF59, ORF60, ORF61, and ORF71), phage structure (ORF4, ORF23, ORF25, ORF48, and ORF53), phage assembly (ORF72), and phage lysis (ORF10) are shown in Fig. 3a. Genes related to the structural components of the phage as well as its assembly and lysis module exhibited consistent transcription orientation.

The BLASTn analysis revealed that phage vB_KpnS_ZX4 exhibited the highest sequence similarity to MZ836210 *Klebsiella* phage BUCT541 (86 % coverage, 97 % identity), followed by NC_054652 Klebsiella phage YX3973 (66 % coverage, 97.23 % identity), MT682064 *Klebsiella* virus KpV2811 (78 % coverage, 95 % identity), JF974294 *Vibrio* phage pYD38-A (69 % coverage, 89 % identity), JF974294 *Aeromonas* phage pIS4-A (69 % coverage, 89 % identity), and MZ318367 *Klebsiella* phage BUCT610 (68 % coverage, 89 % identity) (Fig. 3b). These phages share similar genome size and structure. Phages vB_KpnS_ZX4, BUCT541, and BUCT610 exhibit comparable morphology, with an icosahedral head measuring between 51 and 57 nm in diameter and a tail length of approximately 150 nm. The high sequence similarity of the tail structural proteins (99 %) is closely associated with their morphological resemblance. The tail fiber protein (ORF53) of phage vB_KpnS_ZX4 exhibits a high homology (95 %) with that of BUCT541, KpV2811, and YX3973, suggesting potential similarities in host specificity among these phages. Notably, phage BUCT541 has been reported to selectively lyse ST23 strains of K1 type *K. pneumoniae* (Pu et al., 2022b). In this study, we observed that phage vB_KpnS_ZX4 effectively lyse ST256 strains of K1 type *K. pneumoniae* O4 but not ST367 strains of K1 type *K. pneumoniae* AD1. These findings imply that these phages might recognize different polysaccharide sites within the K1 capsule as receptor.

To analyze the evolutionary relationship of phage vB_KpnS_ZX4, an evolutionary tree was created using the whole genome of phage or the phage terminase large subunits. Fig. S2 show that phage vB_KpnS_ZX4 and the other 9 phages belong to the unclassified *Caudoviricetes*. Among them, the phages vB_KpnS_ZX4, BUCT541, YX3973 and BUCT610 had a close evolutionary relationship.

Table 1
Lytic range of phage vB_KpnS_ZX4.

Klebsiella pneumoniae	Capsular serotype	Virulence gene	Drug resistance gene	Lytic activity of vB_KpnS_ZX4
O4	K1	*rmpA, allS, ureA, fim, iroNB, kfuBC, wabG, wcaG*	*SHV-1*	+
AD1	K1	*rmpA, fim, ybtA, kfuBC, wabG, wcaG*	*SHV-1*	–
602–2	K3	*rmpA, allS, wabG, wcaG*	*SHV-1*	–
N1	K20	*fimH, kfuBC*	*SHV-1*	–
YM2	K20	*fimH, ybtA, kfuBC*	*SHV-1*	–
A1	K54	*fimH, KfuBC*	*SHV-1*	–
N3	K57	*rmpA, iucB, fimH, kfuBC, wabG*	*SHV-1*	–
111–2	K57	*rmpA, allS, iucB, ureA, fim, ybtA, wcaG*	*SHV-187*	–

3.4. Sequence analysis of endolysin LysZX4

The endolysin LysZX4 (ORF10) from phage vB_KpnS_ZX4 is composed of 145 amino acids, with a molecular weight of 15.6 KDa and theoretical isoelectric point (pI) of 9.54. No transmembrane domains or signal peptide sequences were predicted for LysZX4. Secondary structure predictions revealed that LysZX4 consists of 54 % α-spiral, 8 % β-folding, and 6 % irregular crimping. Conservative domain analysis identified that LysZX4 belongs to the lysozyme family (domain architecture ID 10,091,405), which hydrolyzes the (1->4)-β-linkages between N-acetylmuramic acid and N-acetyl-d-glucosamine residues in peptidoglycan. Three-dimensional structure simulation indicated that LysZX4 shares the highest structural similarity with muramidase (confidence, 100 %; identity, 50 %) from *Acinetobacter baumannii* ab 5075uw2 prophage, and a three-dimensional structure was constructed using model c6et6A. Residues at positions 11, 12, 15–17, 34–36, 38–43, 47, 49, 54, 55, 57–59, and 61 were predicted to form catalytic pockets within LysZX4's structure. Phylogenetic analysis demonstrated that LysZX4 (YP 010,054,503) has a close evolutionary relationship with endolysins QWX10285, QZD26122, QYW02896, and URY99550 (Fig. 4a). Amino acid sequence alignment revealed seven differing residues between QWX10285, QZD26122, QYW02896, and URY99550: A39T, S41I, A52V, S74A, S108A, C109R, and Q141E (Fig. 4b), with residue S41 being part of previously predicted catalytic sites. We tested the antibacterial activity of LysZX4 and studied the effects of the above seven amino acids changes on its activity.

3.5. Endolysin expression and purification

After PCR amplification and Sanger sequencing, the endolysin genes LysZX4, LysZX4–39/41 (A39T, S41I), LysZX4–52 (A52V), LysZX4–74 (S74A), LysZX4–108/109 (S108A, C109R), LysZX4–141 (Q141E), LysZX4-NCA (residues KWKLFKI displayed at the N-terminus of LysZX4) and LysZX4-CCA (residues KWKLFKI displayed at the C-terminus of LysZX4) were cloned into the pET28a plasmid. Additionally, both LysZX4 and LysZX4-NCA were cloned into the pET32a plasmid as shown in Fig. S3. The expression of endolysin was achieved in *E. coli* BL21 (DE3) cells, followed by purification. SDS-PAGE analysis resulting in a single band confirmation as observed in Fig. 5a–c and western blot

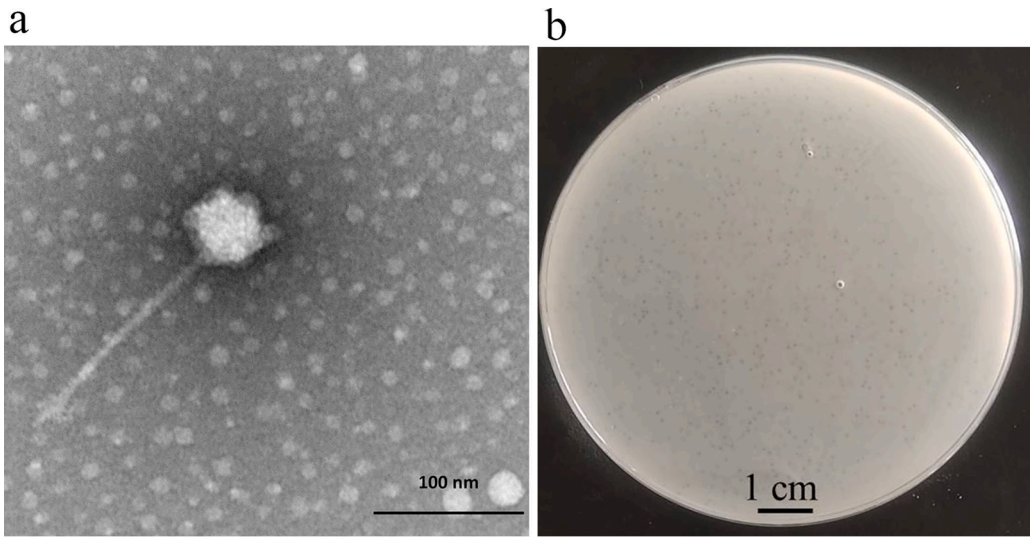

Fig. 1. Morphology of phage vB_KpnS_ZX4. (**a**) TEM picture and (**b**) plaques.

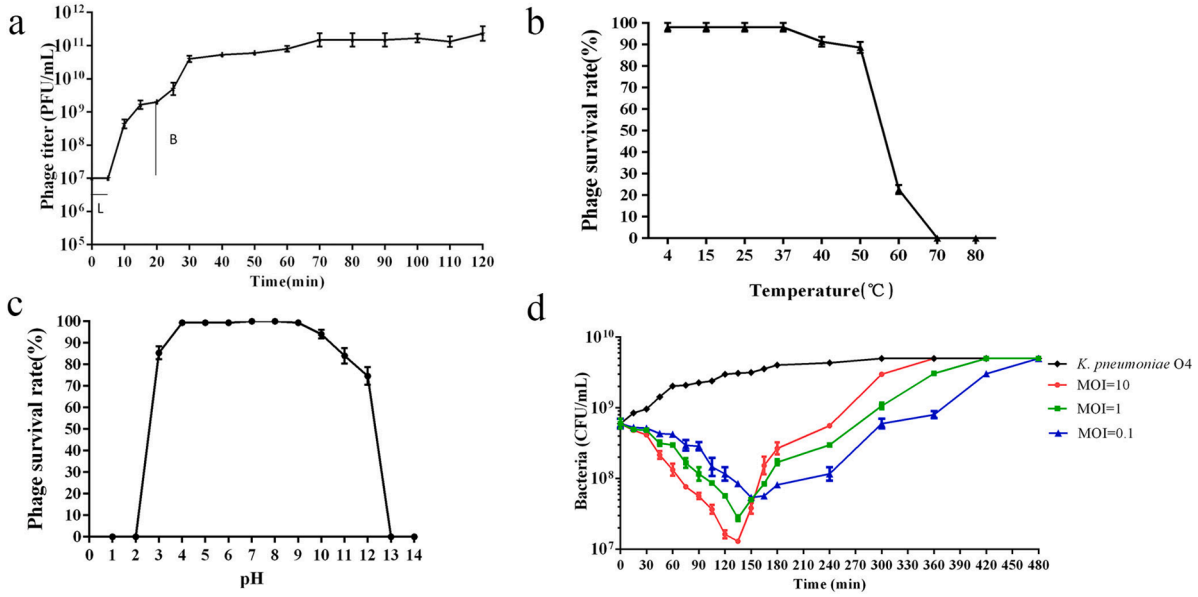

Fig. 2. Biological properties of phage vB_KpnS_ZX4. (**a**) One-step growth curve; (**b**) thermal tolerance; (**c**) pH sensitivity; and (**d**) killing curve *in vitro*.

analysis as depicted in Fig. 5d. Notably, based on the Fig. 5 it can be concluded that when expressed using the pET28a vector system, endolysins have a molecular weight ranging from 20 to 21 kDa; whereas when expressed using the pET32a vector system they exhibit a molecular weight range between 33.2 and 34.2 kDa, respectively. Furthermore, apart from its own inherent sequence consisting of 146 amino acids with a mass of 18.4 kDa, the recombinant endolysin produced via plasmids from the pET28a or pET32a vector carries the his/trx tag at the N-terminus. The main difference between pET28a and pET32a is that pET32a encode an additional trx tag at the N-terminus with 109 amino acids.

3.6. *In vitro* antibacterial activity of endolysin

In vitro antibacterial experiments showed that LysZX4 alone had no antibacterial activity on log-phase *K. pneumoniae* O4, but it had antibacterial activity when used in combination with EDTA (Fig. 6a). After 6 h of LysZX4 (100 μg/mL) combined with 1 mM EDTA treatment, the number of bacteria decreased from 5×10^8 to 7×10^4 CFU/mL. The antibacterial activity of LysZX4 against log-phase *K. pneumoniae* O4 combined with 1 mM EDTA exhibited a concentration-dependent pattern (Fig. 6b). Regarding the minimum effective antibacterial dose of LysZX4 combined with EDTA, the experimental results showed that the bacteria titer of 0.5 mM EDTA and LysZX4 (2.5 μg/mL) 6 h post-administration still decreased significantly from 5×10^8 to 1×10^8 CFU/mL. We also investigated the effect of point mutations on LysZX4 activity. Seven different residues, A39T, S41I, A52V, S74A, S108A, C109R and Q141E, are found in endolysins with high sequence similarity to LysZX4 (Fig. 4b). Our results showed that the mutants of LysZX4 with different mutation site (namely LysZX4–39/41, LysZX4–52, LysZX4–74, LysZX4–108/109, and LysZX4–141) had similar activity to LysZX4 (Fig. 6c). In addition, significant antibacterial activity was initially observed for LysZX4-NCA and was enhanced by the addition of EDTA (Fig. 6d). LysZX4 expressed by the vector pET-28a has a higher antibacterial activity than pET-32a, similar to LysZX4-NCA. The antibacterial activity of LysZX4-NCA in the log phase was higher than that in

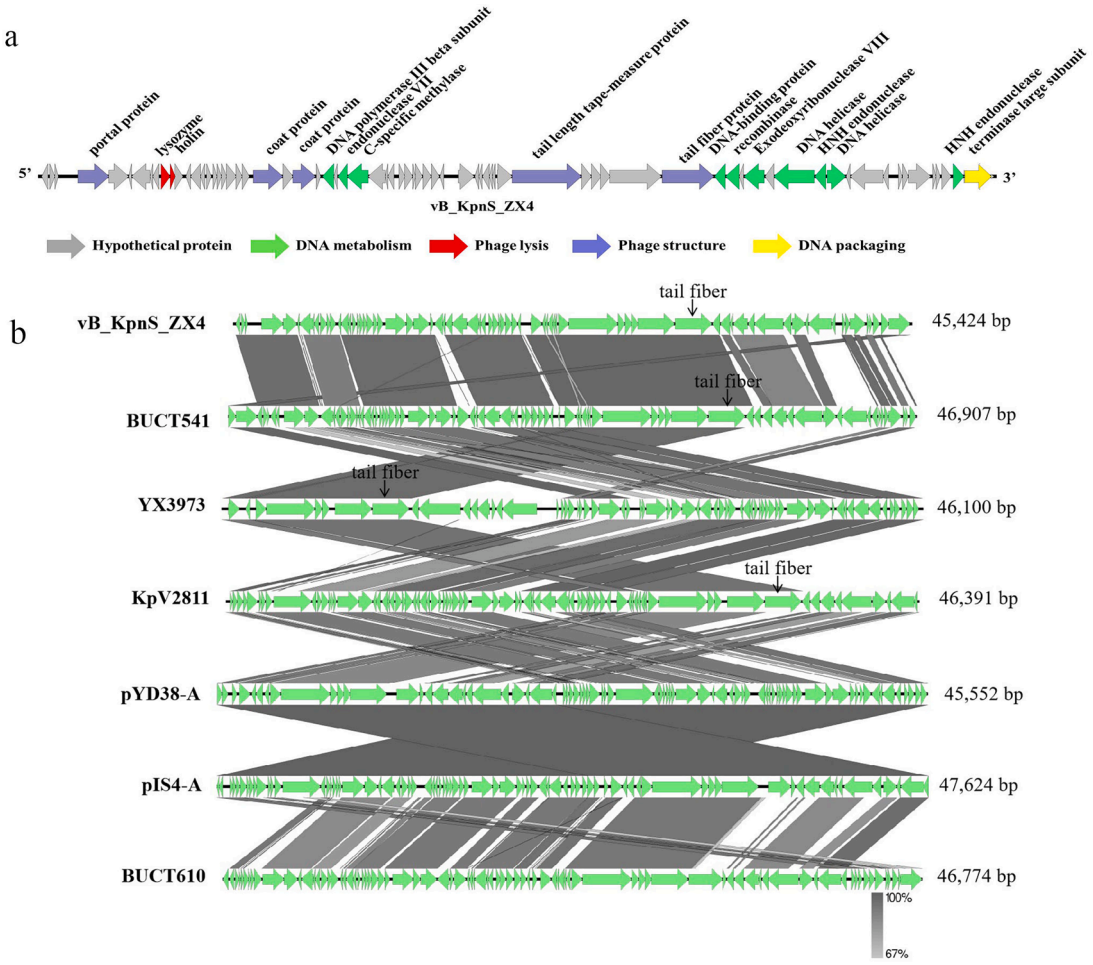

Fig. 3. Genomic analysis of phage vB_KpnS_ZX4. (**a**) Genomic map of phage vB_KpnS_ZX4; (**b**) whole genome alignment and comparison between the phage vB_KpnS_ZX4 and closely related phages.

the stationary phase (Fig. 6e). In a panel of 16 clinical isolates, combination treatment with 1 mM EDTA and LysZX-NCA displayed lytic activity against four strains each of *K. pneumoniae* and *E. coli*, three strains of *P. mirabilis*, as well as four strains of *Citrobacter* (Fig. 6f).

3.7. TEM analysis of endolysin-treated K. pneumoniae

The morphological characteristics of the LysZX4, LysZX4-NCA and PBS-treated cells were significantly different, as observed by TEM. *K. pneumoniae* O4 in control group exhibited smooth surfaces and had an average length of approximately 1.7 ± 0.2 μm long (Fig. 7a). No significant difference in bacterial morphology was observed between the EDTA-treated and control groups (Fig. 7b). However, treatment with LysZX4 (Fig. 7c, d) or LysZX4-NCA (Fig. 7e and f) resulted in osmotic lysis of *K. pneumoniae* O4 cells, leading to the collapse of cell structures and abundant cellular debris formation. Similar observations have been reported for the engineered endolysin LoGT-008, where round or lemon-shaped globular bodies were seen prior to complete dissolution of cells, providing evidence for peptidoglycan degradation (Briers et al., 2014). Artilysin LoGT-008 is designed as an OM-penetrating endolysin that exhibits high bactericidal activity against Gram-negative pathogens. It consists of a fusion between a polycationic nonapeptide and the endolysin PVP-SE1gp146, which can reduce bacteria counts by 4–5 logs within 30 min *in vitro* (Briers et al., 2014).

3.8. Stability of endolysin LysZX4-NCA

The activity of LysZX4-NCA remained stable following treatment at 30, 37, 45, 55, and 65 °C for 1 h; however, it exhibited a decrease to approximately 70 % after exposure to a temperature of 75 °C for the same duration (Fig. 8a). At pH levels of from 6.0 to 9.0, the activity of LysZX4-NCA remained unchanged; nevertheless, it experienced reductions to approximately 7 %, 30 %, 45 %, 83 %, and 50 % at pH values of 3.0, 4.0, 5.0, 10 and 11, respectively (Fig. 8b). The activity of LysZX4-NCA was inhibited by Mg^{2+}, Ca^{2+} and Fe^{2+}, with reductions in activity observed as follows: approximately 86 %, 13 %, 1 % with 0.1, 1, 10 mM Mg^{2+}, respectively; approximately 96 % and 13 % with 1 and 10 mM Ca^{2+} respectively; and approximately 96 % with 10 mM Fe^{2+} (Fig. 8c). The antibacterial activity of LysZX4-NCA did not show any changes when exposed to low concentrations of serum (1–10 %), while 68 % of the activity was retained when exposed to 20 % serum. However, it was completely lost when exposed to 50 % serum.

3.9. In vivo antibacterial activity of vB_KpnS_ZX4 and LysZX4-NCA

No adverse reactions were observed in mice injected with phages, indicating the safety of vB_KpnS_ZX4 for systemic therapy. Following infection with 10^7 CFU of *K. pneumoniae* O4, the bacteria rapidly disseminated to the bloodstream and major organs in mice, reaching a concentration of 10^5 CFU/g after 1 h post-injection and increasing to 10^9 CFU/g after 12 h (Fig. 9a). The rapid proliferation of bacteria resulted in the gradual development of diarrhea, lethargy, and impaired movement

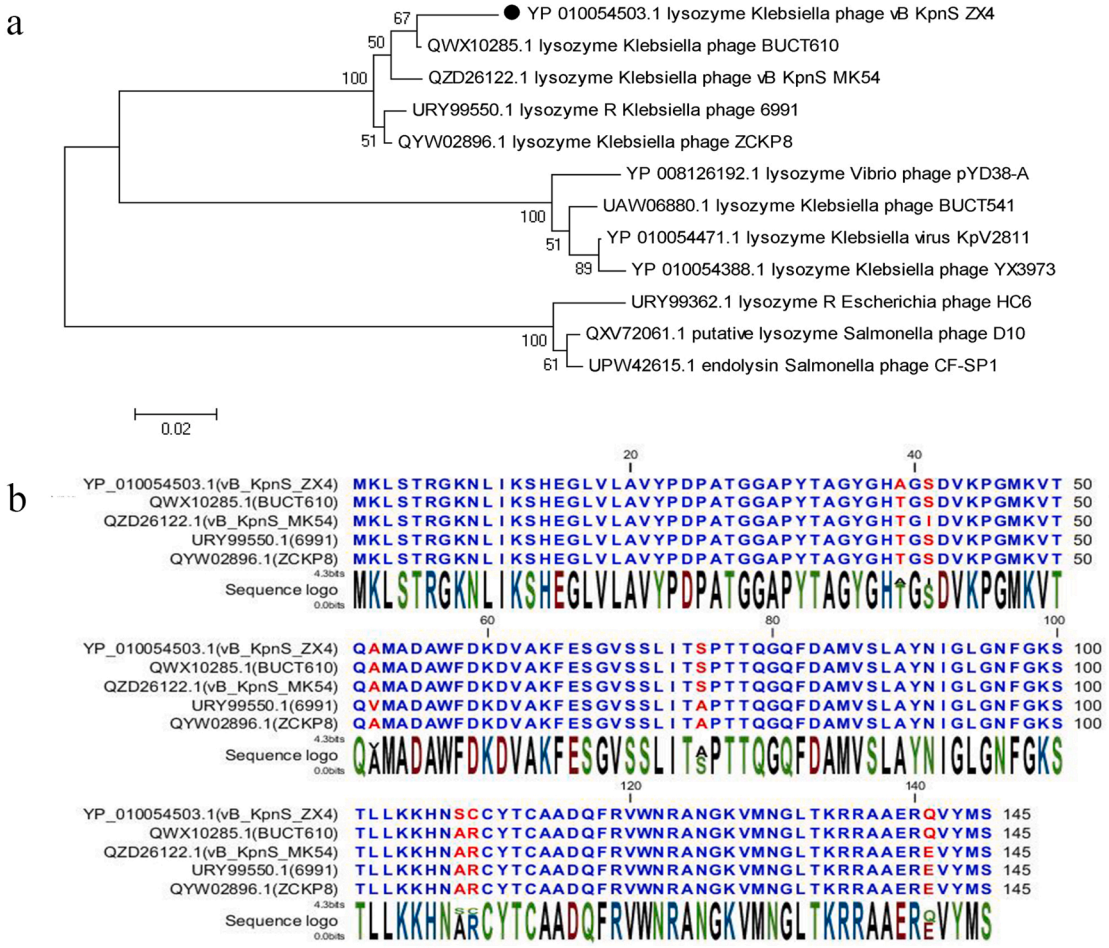

Fig. 4. Amino acid analyses of endolysin LysZX4. (a) Phylogenetic tree; (b) amino acid alignment diagram, with different amino acids are marked in red.

in mice, ultimately leading to mortality after 24 h. Mice treated with intraperitoneal injection of 10^8 PFU vB_KpnS_ZX4 demonstrated effective protection against bacteremia. The survival rates of mice rescued at 1, 3, and 6 h post-infection was 80 %, 60 %, and 0, respectively (Fig. 9b). The bacteria load in blood and organs of surviving mice significantly decreased to 10^3 CFU/g after 24 h and completely cleared after 48 h (Fig. 9c). Since phages only have effective antibacterial activity for 2 h *in vitro*, the immune system plays an important role in the survival of the mice. However, the bacterial burden reached a very high level (10^8 CFU/g) after 6 h of infection, and the available phages were not sufficient to thoroughly eliminate the bacteria, resulting in treatment failure. In a mouse skin infection model, LysZX4-NCA exhibited potent antibacterial activity. After 4 h of treatment, the bacterial count in the treatment group exhibited a significant reduction of 3-log compared to that of the control group (Fig. 9d).

4. Discussion

The phages vB_KpnS_ZX4 and its corresponding phages belong to the unclassified *Caudoviricetes*, potentially constituting a new family. Phages vB_KpnS_ZX4, BUCT541, and BUCT610 display a comparable morphology, characterized by icosahedral capsids and long, non-contractile tails (Pu et al., 2022a, 2022b). Phage vB_KpnS_ZX4 exhibits a shorter latent period (5 min) and lysis period (20 min) compared to BUT541 (30 min and 50 min) and BUCT610 (30 min and 60 min). *In vitro* bactericidal activity assays demonstrated that the addition of vB_KpnS_ZX4 significantly reduced bacterial counts, while the growth trend of bacteria was only inhibited upon addition of BUT541 and BUCT610. The number of bacteria was controlled in a short time after the above-mentioned phages were added but increased again 2 h later. The emergence of resistant strains during late stage of phage application is one of the primary reasons for the failure of phage therapy. Several strategies could be employed to minimize the likelihood of phage resistance, such as phages cocktail and phage domestic modification. Additionally, these phages have been reported to have potent antibacterial activity against *K. pneumoniae in vivo*. Both BUT541 and BUT610 demonstrated effective protective effects in mouse pneumonia models through inhalation or injection, respectively. Furthermore, this study highlights that phage vB_KpnS_ZX4 exhibited significant protective action in a mouse bacteremia model when administered via injection.

Most Gram-negative endolysins are globular structures containing only enzyme activity domains (EADs), while a few have cell binding domains (CBDs) (Briers et al., 2007; Walmagh et al., 2012). CBDs specifically bind enzymes to cell walls and facilitate OM penetration, whereas EADs are responsible for peptidoglycan degradation in cell walls (Vaara, 1992). Endolysins can be categorized into five categories based on their mode of action: N-acetyl-β-d-muramidases, transglycosylases, N-acetyl-β-d-glucosaminidases, N-acetylmuramoyl-l-alanine amidases and endopeptidases (Schmelcher et al., 2012a). LysZX4, QWX10285, LysG24, QYW02896, and URY99550 belong to the group of N-acetyl-β-d-muramidase that cleaves N-acetylmuramoyl-β−1,4-N-acetylglucosamine bonds. The five endolysins exhibit seven amino acids differences among these endolysins reported here. Among the five endolysins, LysG24 (QZD26122, the endolysin of vB_KpnS_MK54) expressed by the pET32a vector has been reported to exhibit antibacterial activity (Lu et al., 2022). Our findings

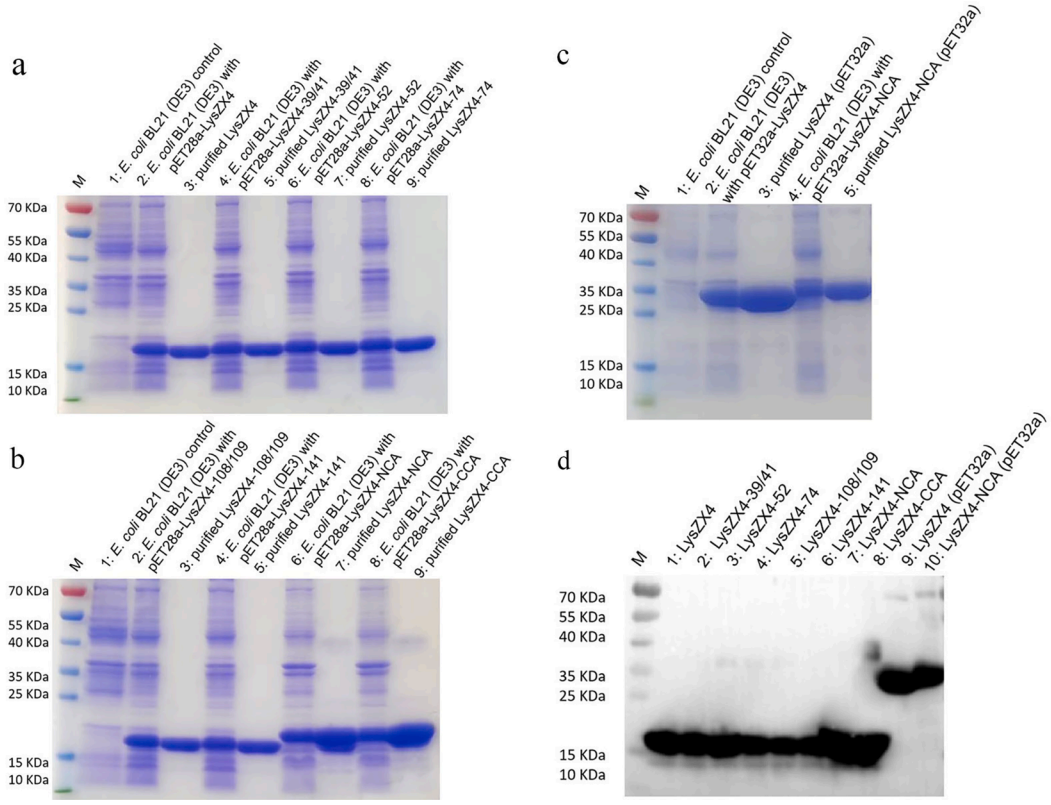

Fig. 5. Expression and purification of endolysin LysZX4. (a/b/c) The SDS-PAGE image of recombinant endolysin; (d) the western blot image of purified endolysin. The sample name of the swim lane has been marked on the image.

reveal that LysZX4 expressed by the pET28a vector exhibits significantly higher antibacterial activity compared to its expression using the pET32a vector. This difference may be attributed to the presence of the trx tag carried pET-32a which might hinder its functionality.

LysZX4 exhibits antibacterial activity against cells in both the log and stationary phases only in the presence of an OM penetrant. Due to the presence of an OM, LysZX4 cannot access peptidoglycan, resulting in no antibacterial activity even at high concentrations. However, it shows activity in the presence of a small amount of OM penetrant EDTA. The addition of EDTA can effectively remove divalent ions that stabilize the cell surface structure, leading to destabilization of the OM. However, its application is limited due to its coagulation characteristics (Briers et al., 2011). Organic acids such as citric acid and malic acid are more suitable for combination with endolysin for *in vivo* antibacterial therapy (Oliveira et al., 2014). The antibacterial activity of LysZX4 against bacteria in the log phase was significantly higher compared to the stationary phase bacteria. This finding is consistent with previous reports, which suggest that differences in the complex structure and content of the OM and peptidoglycan contribute to this variation among bacterial growth phases (Lood et al., 2015; Raz et al., 2019). In addition to OM permeabilizers, incorporating peptides into the endolysin can also effectively enhance its antibacterial activity, including membrane-penetrating peptides (Briers et al., 2011), membrane translocating domains (Heselpoth et al., 2019), and polycationic nonapeptide (Briers et al., 2014). Modification of LysZX4-NCA/CCA with the cecropin A residue resulted in higher antibacterial activity compared to unmodified LysZX4, with N-terminal modification showing superior efficacy over C-terminal modification. Previous studies have shown that N-terminal fusion exhibits greater antibacterial activity than C-terminal fusion, while increasing the length of the linker between labels and endolysins can also improve their antibacterial effectiveness (Briers et al., 2014). Furthermore, LysZX4-NCA combined with EDTA demonstrated a broad antibacterial spectrum against *K. pneumoniae, E. coli, P. mirabilis*, and *Citrobacter*. The lytic spectrum of a N-acetyl-β-d-muramidase is typically broad, because the polysaccharide backbone is the most conserved part of the murein (Walmagh et al., 2012). Endolysins with alternative enzymatic activities can exhibit high specificity towards species or subspecies.

LysZX4-NCA exhibits a high temperature resistance ranging from 30 to 65 °C. While most endolysins maintain stability within the range of 30–40 °C, a few have been reported to remain stable even at higher temperatures such as 80 °C (Shavrina et al., 2016; Walmagh et al., 2012; Yang et al., 2018), and in some cases, up to 90 °C for a duration of 0.5–2 h (Schmelcher et al., 2012b). 10 mM K^+ was shown to inhibit the activity of endolysin to varying degrees by previous study (Antonova et al., 2019). However, this inhibitory effect was not observed for LysZX4-NCA. Generally, 1 %−20 % serum can inhibit the activity of endolysins, such as PlyPaO3 and PlyPa91 (Raz et al., 2019). In contrast, the antibacterial activity of LysZX4-NCA was found to be inhibited by 20 % serum and completely lost in 50 % serum. These findings suggest that while these endolysins may be not suitable for systemic use, they hold promise for topical applications, such as treating lung and skin infections. Notably, previous studies have demonstrated that LysG24 significantly reduces the bacterial titers in pneumonia model, whereas our study reveals that LysZX4-NCA significantly reduces the bacterial titers in skin model.

5. Conclusions

In this study, the novel lytic phage vB_KpnS_ZX4 was isolated against MDR-hvKP. Phage vB_KpnS_ZX4 exhibited rapid bactericidal activity both *in vivo* and *in vitro,* significantly reducing the mortality rate of mice with bacteremia. Furthermore, the endolysin LysZX4 from vB_KpnS_ZX4 demonstrated potent antibacterial activity when combined with EDTA *in vitro*. To enhance its efficacy, LysZX4-NCA was further augmented by fusing KWKLFKI residues. Notably, LysZX4-NCA displayed broad-

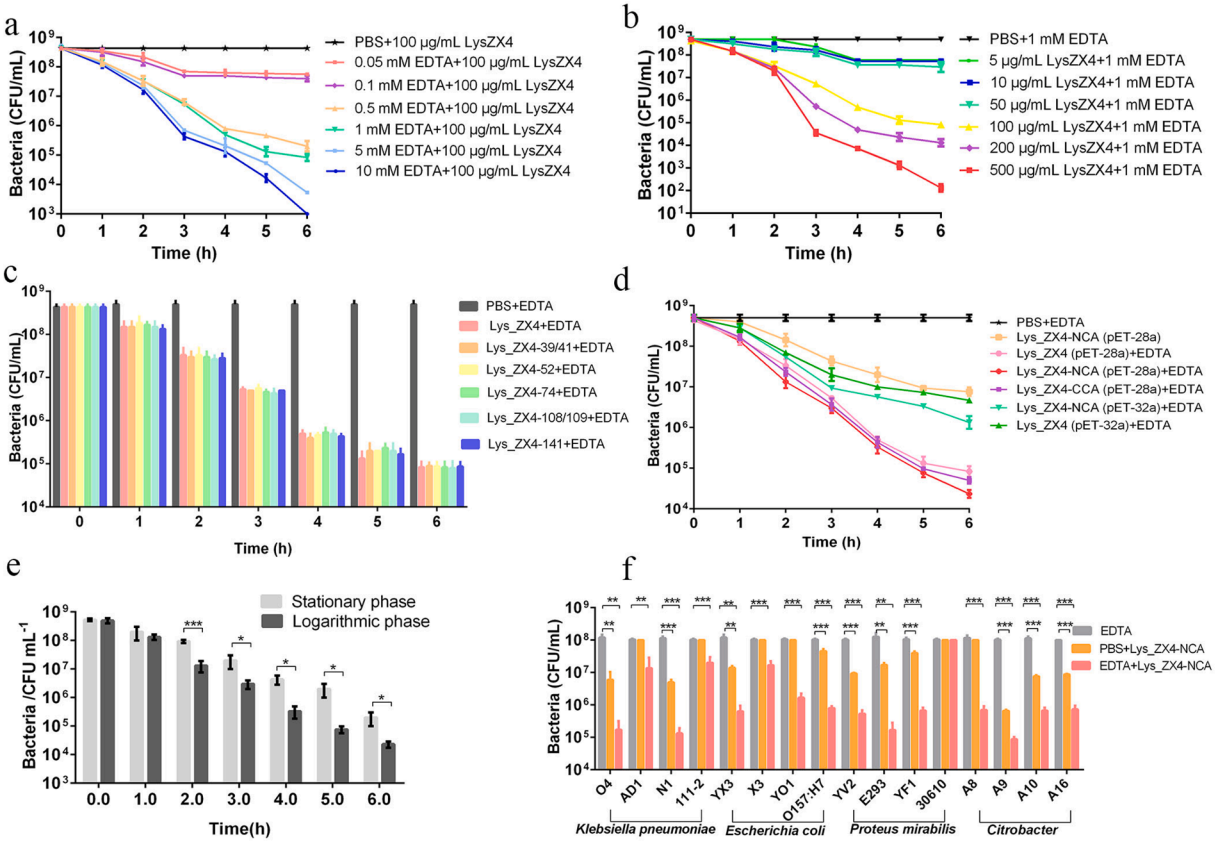

Fig. 6. Antibacterial activities of endolysin LysZX4 *in vitro*. (a) Antibacterial activities of LysZX4 with different concentrations of EDTA; (b) antibacterial activities of 1 mM EDTA combined with LysZX4 in different concentrations; (c) antibacterial activities of LysZX4 mutants combined with 1 mM EDTA; (d) antibacterial activities of engineered LysZX4 combined with 1 mM EDTA; (e) antibacterial activities of LysZX4 combined with 1 mM EDTA to log-phase and stationary-phase; and (f) antibacterial activities of LysZX4-NCA combined with 1 mM EDTA for clinical isolates.

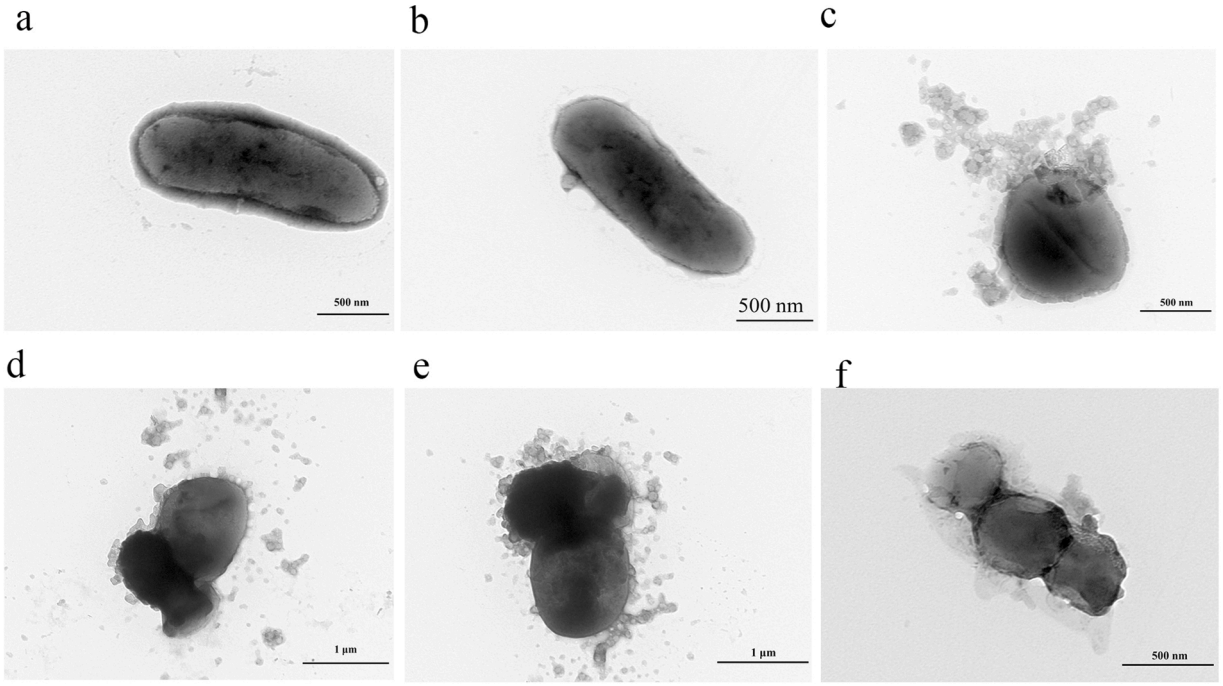

Fig. 7. TEM pictures of endolysin-treated *K. pneumoniae* O4. (a) Log-phase *K. pneumoniae* O4; (b) log-phase *K. pneumoniae* O4 treated with EDTA; (c/d) log-phase *K. pneumoniae* O4 treated with LysZX4; (e/f) log-phase *K. pneumoniae* O4 treated with LysZX4-NCA.

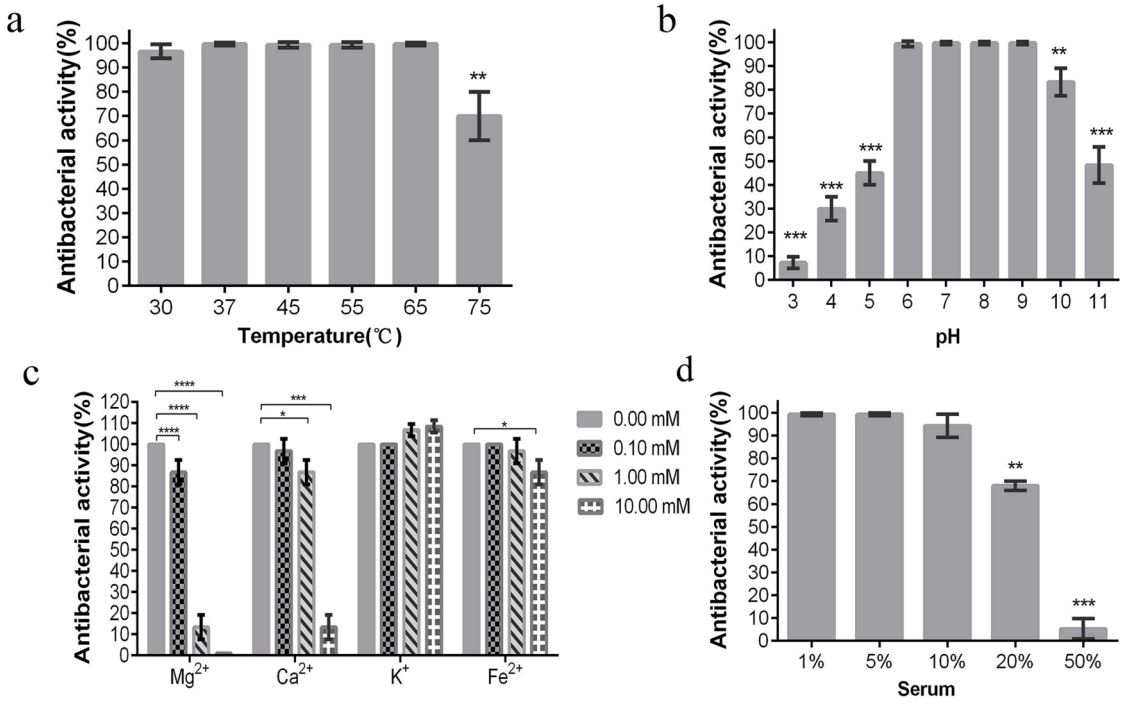

Fig. 8. Stability tests of endolysin LysZX4-NCA. (a) Temperature stability; (b) pH stability; (c) metal ion stability; and (d) serum stability.

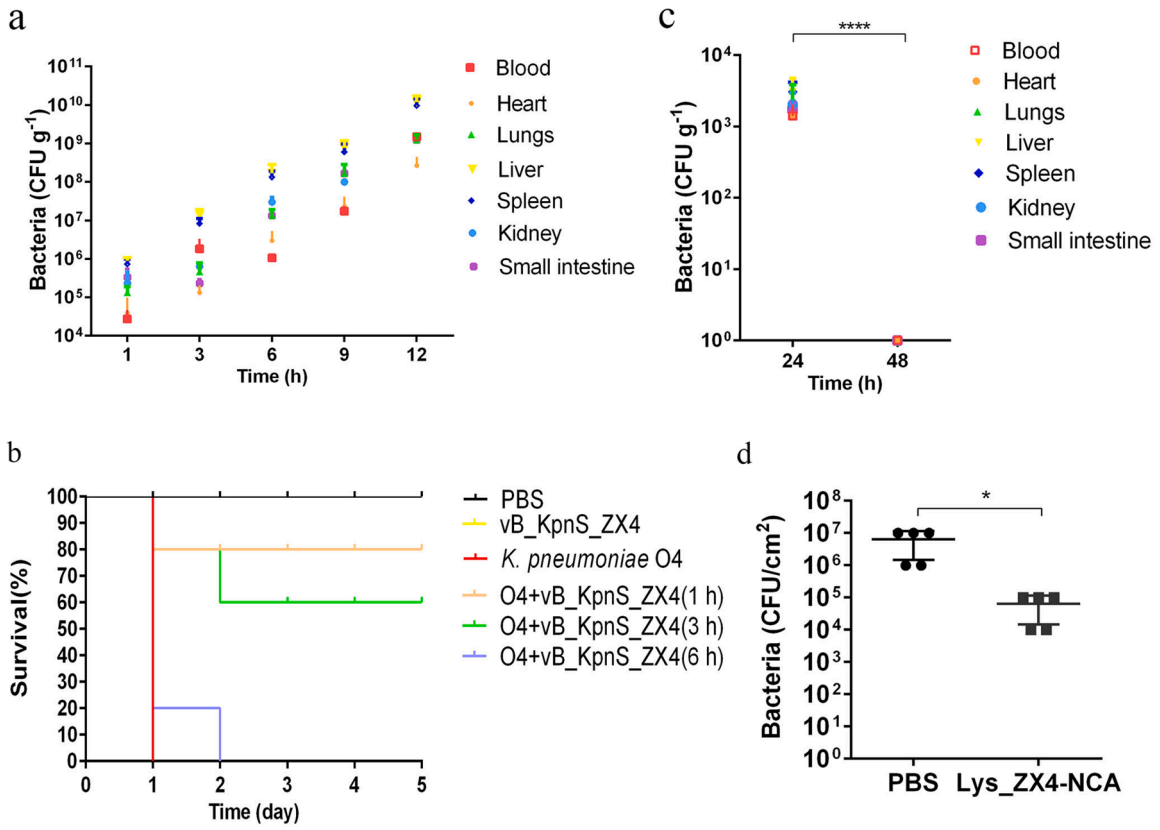

Fig. 9. Antibacterial activities vB_KpnS_ZX4 and LysZX4-NCA *in vivo*. (a) Number of bacteria in mice with bacteremia; (b) survival rates of mice after vB_KpnS_ZX4 therapy in the model of bacteremia; (c) number of bacteria after vB_KpnS_ZX4 therapy in surviving mice; and (d) number of bacteria after LysZX4-NCA treatment in mouse skin infection model.

spectrum bactericidal effects against clinical strains of Gram-negative bacteria including *K. pneumoniae, E. coli, P. mirabilis*, and *Citrobacter*. In a mouse skin infection model, LysZX4-NCA exhibited effective antibacterial effects and is considered suitable for topical treatment. Collectively, our findings highlight the potential of phages vB_KpnS_ZX4 and LysZX4-NCA as promising alternatives to antibiotic therapy.

Funding

This research was funded by the National Natural Science Foundation of China (grant number: 32271435), Shanghai Science and Technology Innovation Action Plan in 2022 (grant number: 22N31900800), and Priority Academic Program Development of Jiangsu Higher Education Institutions (PAPD).

Institutional review board statement

The study was approved by the Animal Welfare and Research Ethics Committee of Yangzhou University (202103440l).

Informed consent statement

Not applicable.

CRediT authorship contribution statement

Ping Li: Conceptualization, Data curation, Formal analysis, Investigation, Methodology, Validation, Writing – original draft. **Mangmang Shen:** Methodology, Validation. **Wenjie Ma:** Formal analysis, Investigation, Methodology, Validation. **Xin Zhou:** Conceptualization, Funding acquisition, Project administration, Resources, Supervision, Writing – review & editing. **Jiayin Shen:** Conceptualization, Project administration, Supervision, Writing – review & editing.

Declaration of Competing Interest

The authors declare that they have no known competing financial interests or personal relationships that could have appeared to influence the work reported in this paper.

Data availability

No data was used for the research described in the article.

Supplementary materials

Supplementary material associated with this article can be found, in the online version, at doi:10.1016/j.virusres.2023.199296.

References

Alcock, B.P., Raphenya, A.R., Lau, T.T.Y., Tsang, K.K., Bouchard, M., Edalatmand, A., Huynh, W., Nguyen, A.V., Cheng, A.A., Liu, S., Min, S.Y., Miroshnichenko, A., Tran, H.K., Werfalli, R.E., Nasir, J.A., Oloni, M., Speicher, D.J., Florescu, A., Singh, B., Faltyn, M., Hernandez-Koutoucheva, A., Sharma, A.N., Bordeleau, E., Pawlowski, A.C., Zubyk, H.L., Dooley, D., Griffiths, E., Maguire, F., Winsor, G.L., Beiko, R.G., Brinkman, F.S.L., Hsiao, W.W.L., Domselaar, G.V., McArthur, A.G., 2020. CARD 2020: antibiotic resistome surveillance with the comprehensive antibiotic resistance database. Nucl. Acid. Res. 48 (D1), D517–d525.

Anand, T., Virmani, N., Kumar, S., Mohanty, A.K., Pavulraj, S., Bera, B.C., Vaid, R.K., Ahlawat, U., Tripathi, B.N., 2020. Phage therapy for treatment of virulent Klebsiella pneumoniae infection in a mouse model. J. Glob. Antimicrob. Resist. 21, 34–41.

Antonova, N.P., Vasina, D.V., Lendel, A.M., Usachev, E.V., Makarov, V.V., Gintsburg, A. L., Tkachuk, A.P., Gushchin, V.A., 2019. Broad bactericidal activity of the myoviridae bacteriophage lysins LysAm24, LysECD7, and LysSi3 against Gram-negative ESKAPE pathogens. Viruses 11 (3).

Briers, Y., Volckaert, G., Cornelissen, A., Lagaert, S., Michiels, C.W., Hertveldt, K., Lavigne, R., 2007. Muralytic activity and modular structure of the endolysins of Pseudomonas aeruginosa bacteriophages phiKZ and EL. Mol. Microbiol. 65 (5), 1334–1344.

Briers, Y., Walmagh, M., Lavigne, R., 2011. Use of bacteriophage endolysin EL188 and outer membrane permeabilizers against Pseudomonas aeruginosa. J. Appl. Microbiol. 110 (3), 778–785.

Briers, Y., Walmagh, M., Van Puyenbroeck, V., Cornelissen, A., Cenens, W., Aertsen, A., Oliveira, H., Azeredo, J., Verween, G., Pirnay, J.P., Miller, S., Volckaert, G., Lavigne, R., 2014. Engineered endolysin-based "Artilysins" to combat multidrug-resistant gram-negative pathogens. mBio 5 (4) e01379-01314.

Calfee, D.P., 2010. Klebsiella pneumoniae carbapenemase-producing Enterobacteriaceae. J. Infus. Nurs. 33 (3), 150–154.

Chamblee, J.S., Ramsey, J., Chen, Y., Maddox, L.T., Ross, C., To, K.H., Cahill, J.L., Young, R., 2022. Endolysin regulation in phage mu lysis. mBio 13 (3), e0081322.

Chan, P.P., Lin, B.Y., Mak, A.J., Lowe, T.M., 2021. tRNAscan-SE 2.0: improved detection and functional classification of transfer RNA genes. Nucl. Acid. Res. 49 (16), 9077–9096.

Fischetti, V.A., 2018. Development of phage lysins as novel therapeutics: a historical perspective. Viruses 10 (6).

Ghose, C., Euler, C.W., 2020. Gram-negative bacterial lysins. Antibiot. (Basel) 9 (2).

Gorodnichev, R.B., Volozhantsev, N.V., Krasilnikova, V.M., Bodoev, I.N., Kornienko, M. A., Kuptsov, N.S., Popova, A.V., Makarenko, G.I., Manolov, A.I., Slukin, P.V., Bespiatykh, D.A., Verevkin, V.V., Denisenko, E.A., Kulikov, E.E., Veselovsky, V.A., Malakhova, M.V., Dyatlov, I.A., Ilina, E.N., Shitikov, E.A., 2021. Novel Klebsiella pneumoniae K23-specific bacteriophages from different families: similarity of depolymerases and their therapeutic potential. Front. Microbiol. 12, 669618.

Hancock, R.E., Chapple, D.S., 1999. Peptide antibiotics. Antimicrob. Agents Chemother. 43 (6), 1317–1323.

Heselpoth, R.D., Euler, C.W., Schuch, R., Fischetti, V.A., 2019. Lysocins: bioengineered antimicrobials that deliver lysins across the outer membrane of Gram-negative bacteria. Antimicrob. Agents Chemother. 63 (6).

Hesse, S., Malachowa, N., Porter, A.R., Freedman, B., Kobayashi, S.D., Gardner, D.J., Scott, D.P., Adhya, S., DeLeo, F.R., 2021. Bacteriophage treatment rescues mice infected with multidrug-resistant Klebsiella pneumoniae ST258. mBio 12 (1).

Ho, M.K.Y., Zhang, P., Chen, X., Xia, J., Leung, S.S.Y., 2022. Bacteriophage endolysins against gram-positive bacteria, an overview on the clinical development and recent advances on the delivery and formulation strategies. Crit. Rev. Microbiol. 48 (3), 303–326.

Hung, C.H., Kuo, C.F., Wang, C.H., Wu, C.M., Tsao, N., 2011. Experimental phage therapy in treating Klebsiella pneumoniae-mediated liver abscesses and bacteremia in mice. Antimicrob. Agent. Chemother. 55 (4), 1358–1365.

Keen, E.C., 2015. A century of phage research: bacteriophages and the shaping of modern biology. Bioessays 37 (1), 6–9.

Kelley, L.A., Mezulis, S., Yates, C.M., Wass, M.N., Sternberg, M.J., 2015. The Phyre2 web portal for protein modeling, prediction and analysis. Nat. Protoc. 10 (6), 845–858.

Kumari, S., Harjai, K., Chhibber, S., 2009. Efficacy of bacteriophage treatment in murine burn wound infection induced by Klebsiella pneumoniae. J. Microbiol. Biotechnol. 19 (6), 622–628.

Lai, W.C.B., Chen, X., Ho, M.K.Y., Xia, J., Leung, S.S.Y., 2020. Bacteriophage-derived endolysins to target gram-negative bacteria. Int. J. Pharm. 589, 119833.

Li, P., Ma, W., Shen, J., Zhou, X., 2022. Characterization of novel bacteriophage vB_KpnP_ZX1 and its depolymerases with therapeutic potential for K57 Klebsiella pneumoniae Infection. Pharmaceutics 14 (9).

Li, P., Zhang, Y., Yan, F., Zhou, X., 2021. Characteristics of a bacteriophage, vB_Kox_ZX8, isolated from clinical Klebsiella oxytoca and its therapeutic effect on mice bacteremia. Front. Microbiol. 12, 763136.

Liu, B., Zheng, D., Jin, Q., Chen, L., Yang, J., 2019. VFDB 2019: a comparative pathogenomic platform with an interactive web interface. Nucl. Acid. Res. 47 (D1), D687–d692.

Lood, R., Winer, B.Y., Pelzek, A.J., Diez-Martinez, R., Thandar, M., Euler, C.W., Schuch, R., Fischetti, V.A., 2015. Novel phage lysin capable of killing the multidrug-resistant gram-negative bacterium Acinetobacter baumannii in a mouse bacteremia model. Antimicrob. Agent. Chemother. 59 (4), 1983–1991.

Lu, B., Yao, X., Han, G., Luo, Z., Zhang, J., Yong, K., Wang, Y., Luo, Y., Yang, Z., Ren, M., Cao, S., 2022. Isolation of Klebsiella pneumoniae phage vB_KpnS_MK54 and pathological assessment of endolysin in the treatment of pneumonia mice model. Front. Microbiol. 13, 854908.

Lu, S., Wang, J., Chitsaz, F., Derbyshire, M.K., Geer, R.C., Gonzales, N.R., Gwadz, M., Hurwitz, D.I., Marchler, G.H., Song, J.S., Thanki, N., Yamashita, R.A., Yang, M., Zhang, D., Zheng, C., Lanczycki, C.J., Marchler-Bauer, A., 2020. CDD/SPARCLE: the conserved domain database in 2020. Nucl. Acid. Res. 48 (D1), D265–D268.

Maciejewska, B., Roszniowski, B., Espaillat, A., Kęsik-Szeloch, A., Majkowska-Skrobek, G., Kropinski, A.M., Briers, Y., Cava, F., Lavigne, R., Drulis-Kawa, Z., 2017. Klebsiella phages representing a novel clade of viruses with an unknown DNA modification and biotechnologically interesting enzymes. Appl. Microbiol. Biotechnol. 101 (2), 673–684.

Martin, R.M., Bachman, M.A., 2018. Colonization, infection, and the accessory genome of Klebsiella pneumoniae. Front. Cell. Infect. Microbiol. 8, 4.

Oliveira, H., Thiagarajan, V., Walmagh, M., Sillankorva, S., Lavigne, R., Neves-Petersen, M.T., Kluskens, L.D., Azeredo, J., 2014. A thermostable Salmonella phage endolysin, Lys68, with broad bactericidal properties against gram-negative pathogens in presence of weak acids. PLoS One 9 (10), e108376.

Overbeek, R., Olson, R., Pusch, G.D., Olsen, G.J., Davis, J.J., Disz, T., Edwards, R.A., Gerdes, S., Parrello, B., Shukla, M., Vonstein, V., Wattam, A.R., Xia, F., Stevens, R., 2014. The SEED and the rapid annotation of microbial genomes using subsystems technology (RAST). Nucl. Acid. Res. 42, D206–D214. Database issue.

Pastagia, M., Euler, C., Chahales, P., Fuentes-Duculan, J., Krueger, J.G., Fischetti, V.A., 2011. A novel chimeric lysin shows superiority to mupirocin for skin decolonization of methicillin-resistant and -sensitive Staphylococcus aureus strains. Antimicrob. Agent. Chemother. 55 (2), 738–744.

Podschun, R., Ullmann, U., 1998. Klebsiella spp. as nosocomial pathogens: epidemiology, taxonomy, typing methods, and pathogenicity factors. Clin. Microbiol. Rev. 11 (4), 589–603.

Pu, M., Han, P., Zhang, G., Liu, Y., Li, Y., Li, F., Li, M., An, X., Song, L., Chen, Y., Fan, H., Tong, Y., 2022a. Characterization and comparative genomics analysis of a new bacteriophage BUCT610 against Klebsiella pneumoniae and efficacy assessment in galleria mellonella larvae. Int. J. Mol. Sci. 23 (14).

Pu, M., Li, Y., Han, P., Lin, W., Geng, R., Qu, F., An, X., Song, L., Tong, Y., Zhang, S., Cai, Z., Fan, H., 2022b. Genomic characterization of a new phage BUCT541 against Klebsiella pneumoniae K1-ST23 and efficacy assessment in mouse and Galleria mellonella larvae. Front. Microbiol. 13, 950737.

Pusparajah, P., Letchumanan, V., Goh, B.H., McGaw, L.J., 2022. Editorial: novel approaches to the treatment of multidrug-resistant bacteria. Front. Pharmacol. 13, 972935.

Qin, J., Wu, N., Bao, J., Shi, X., Ou, H., Ye, S., Zhao, W., Wei, Z., Cai, J., Li, L., Guo, M., Weng, J., Lu, H., Tan, D., Zhang, J., Huang, Q., Zhu, Z., Shi, Y., Hu, C., Guo, X., Zhu, T., 2020. Heterogeneous Klebsiella pneumoniae co-infections complicate personalized bacteriophage therapy. Front. Cell. Infect. Microbiol. 10, 608402.

Raz, A., Serrano, A., Hernandez, A., Euler, C.W., Fischetti, V.A., 2019. Isolation of phage lysins that effectively kill pseudomonas aeruginosa in mouse models of lung and skin infection. Antimicrob. Agents Chemother. 63 (7).

Schmelcher, M., Donovan, D.M., Loessner, M.J., 2012a. Bacteriophage endolysins as novel antimicrobials. Fut. Microbiol. 7 (10), 1147–1171.

Schmelcher, M., Waldherr, F., Loessner, M.J., 2012b. Listeria bacteriophage peptidoglycan hydrolases feature high thermoresistance and reveal increased activity after divalent metal cation substitution. Appl. Microbiol. Biotechnol. 93 (2), 633–643.

Shavrina, M.S., Zimin, A.A., Molochkov, N.V., Chernyshov, S.V., Machulin, A.V., Mikoulinskaia, G.V., 2016. *In vitro* study of the antibacterial effect of the bacteriophage T5 thermostable endolysin on Escherichia coli cells. J. Appl. Microbiol. 121 (5), 1282–1290.

Sullivan, M.J., Petty, N.K., Beatson, S.A., 2011. Easyfig: a genome comparison visualizer. Bioinformatics 27 (7), 1009–1010.

Tang, M., Kong, X., Hao, J., Liu, J., 2020. Epidemiological characteristics and formation mechanisms of multidrug-resistant hypervirulent Klebsiella pneumoniae. Front. Microbiol. 11, 581543.

Tutelyan, A.V., Shlykova, D.S., Voskanyan, S.L., Gaponov, A.M., Pisarev, V.M., 2022. Molecular epidemiology of hypervirulent K. pneumoniae and problems of health-care associated infections. Bull. Exp. Biol. Med. 172 (5), 507–522.

Vaara, M., 1992. Agents that increase the permeability of the outer membrane. Microbiol. Rev. 56 (3), 395–411.

Walmagh, M., Boczkowska, B., Fau - Grymonprez, B., Grymonprez, B., Fau - Briers, Y., Briers, Y., Fau - Drulis-Kawa, Z., Drulis-Kawa, Z., Fau - Lavigne, R., Lavigne, R., 2013. Characterization of five novel endolysins from Gram-negative infecting bacteriophages. Appl. Microbiol. Biotechnol. 97 (10), 4369–4375.

Walmagh, M., Briers, Y., dos Santos, S.B., Azeredo, J., Lavigne, R., 2012. Characterization of modular bacteriophage endolysins from Myoviridae phages OBP, 201φ2-1 and PVP-SE1. PLoS One 7 (5), e36991.

Wang, Z., Cai, R., Wang, G., Guo, Z., Liu, X., Guan, Y., Ji, Y., Zhang, H., Xi, H., Zhao, R., Bi, L., Liu, S., Yang, L., Feng, X., Sun, C., Lei, L., Han, W., Gu, J., 2021. Combination therapy of phage vB_KpnM_P-KP2 and gentamicin combats acute pneumonia caused by K47 serotype Klebsiella pneumoniae. Front. Microbiol. 12, 674068.

Yang, Y., Le, S., Shen, W., Chen, Q., Huang, Y., Lu, S., Tan, Y., Li, M., Hu, F., Li, Y., 2018. Antibacterial activity of a lytic enzyme encoded by pseudomonas aeruginosa double stranded RNA bacteriophage phiYY. Front. Microbiol. 9, 1778.